HHS Public Access

Author manuscript

Brain Struct Funct. Author manuscript; available in PMC 2023 July 05.

Published in final edited form as:

Brain Struct Funct. 2023 May ; 228(3-4): 1019–1031. doi:10.1007/s00429-023-02642-x.

Superficial white matter across development, young adulthood, and aging: volume, thickness, and relationship with cortical features

Kurt G. Schilling[1,2], **Derek Archer**[3,4,5], **Francois Rheault**[6], **Ilwoo Lyu**[7], **Yuankai Huo**[6], **Leon Y. Cai**[8], **Silvia A. Bunge**[9], **Kevin S. Weiner**[9,10], **John C. Gore**[1,2], **Adam W. Anderson**[2,8], **Bennett A. Landman**[1,2,7]

[1] Department of Radiology and Radiological Sciences, Vanderbilt University Medical Center, Nashville, TN, USA

[2] Vanderbilt University Institute of Imaging Science, Vanderbilt University, Nashville, TN, USA

[3] Vanderbilt Memory and Alzheimer's Center, Vanderbilt University Medical Center, Nashville, TN, USA

[4] Department of Neurology, Vanderbilt University Medical Center, Nashville, TN, USA

[5] Vanderbilt Genetics Institute, Vanderbilt University School of Medicine, Nashville, TN, USA

[6] Department of Electrical Engineering and Computer Engineering, Vanderbilt University, Nashville, TN, USA

[7] Computer Science and Engineering, Ulsan National Institute of Science and Technology, Ulsan, South Korea

[8] Department of Biomedical Engineering, Vanderbilt University, Nashville, TN, USA

[9] Department of Psychology, University of California at Berkeley, Berkeley, USA

[10] Helen Wills Neuroscience Institute, University of California at Berkeley, Berkeley, USA

Abstract

Superficial white matter (SWM) represents a significantly understudied part of the human brain, despite comprising a large portion of brain volume and making up a majority of cortico-cortical white matter connections. Using multiple, high-quality datasets with large sample sizes (N = 2421, age range 5–100) in combination with methodological advances in tractography, we quantified features of SWM volume and thickness across the brain and across development, young adulthood, and aging. We had four primary aims: (1) characterize SWM thickness across brain regions (2) describe associations between SWM volume and age (3) describe associations between

✉ Kurt G. Schilling kurt.g.schilling.1@vumc.org.

Author contributions Conceptualization: KS, DA, IL, SB, KW, JG, AA, BLFormal analysis: KS, DA, FR, YH, LCData Curation: KS, DA, FR, LCWriting: KS, DA, BLReviewing and editing: all authors

Conflict of interest The authors have not disclosed any competing interests.

Competing interests The authors declare no competing interests.

Supplementary Information The online version contains supplementary material available at https://doi.org/10.1007/s00429-023-02642-x.

SWM thickness and age, and (4) quantify relationships between SWM thickness and cortical features. Our main findings are that (1) SWM thickness varies across the brain, with patterns robust across individuals and across the population at the region-level and vertex-level; (2) SWM volume shows unique volumetric trajectories with age that are distinct from gray matter and other white matter trajectories; (3) SWM thickness shows nonlinear cross-sectional changes across the lifespan that vary across regions; and (4) SWM thickness is associated with features of cortical thickness and curvature. For the first time, we show that SWM volume follows a similar trend as overall white matter volume, peaking at a similar time in adolescence, leveling off throughout adulthood, and decreasing with age thereafter. Notably, the relative fraction of total brain volume of SWM continuously increases with age, and consequently takes up a larger proportion of total white matter volume, unlike the other tissue types that decrease with respect to total brain volume. This study represents the first characterization of SWM features across the large portion of the lifespan and provides the background for characterizing normal aging and insight into the mechanisms associated with SWM development and decline.

Keywords

Superficial white matter; U-fibers; Tractography; Lifespan; Development; Aging

Introduction

Superficial white matter (SWM) is the layer of white matter immediately beneath the cortex, and is composed of short-range association U-shaped fibers, or U-fibers, that primarily connect adjacent gyri (Guevara et al. 2020). As summarized in Kirilina et al. (2020), these connections are unique, as they occupy a majority of the total white matter volume (Schüz et al. 2002), account for a majority of the cortico-cortical white matter connections of the human brain (Schüz et al. 2002; Schüz and Miller 2002), are among the last parts of the brain to myelinate (Wu et al. 2014; Barkovich 2000; Schuz et al. 2006; Maricich et al. 2007), and contain a relatively high density of neurons relative to other white matter systems (Suarez-Sola et al. 2009). Further, SWM has been shown to play a critical role in brain function, cognition, and disease (Guevara et al. 2020; Kirilina et al. 2020).

Despite its significance, SWM has been critically understudied compared to the long-range projection, association, and commissural fibers of the brain. This is largely attributed to challenges and limitations of diffusion MRI fiber tractography (Guevara et al. 2020; Schilling et al. 2018; Shastin et al. 2022), which is the primary modality used to study the structural connections of the human brain in vivo (Jeurissen et al. 2019). These challenges are associated with the complex anatomy of the SWM, including complex fiber orientation, fiber trajectories with high curvature, and partial volume effects with both gray matter and other white matter systems (Shastin et al. 2022; Reveley et al. 2015). However, recent advances in MRI data acquisition and image processing have made it possible to reliably study SWM in health and disease. This is typically done by measuring diffusion values such as fractional anisotropy (FA), mean diffusivity (MD), axial diffusivity (AD), and/or radial diffusivity (RD), and quantifying their changes in pathology. For example, decreases in anisotropy and increases in diffusivity of SWM have been documented in Alzheimer’s

disease, autism spectrum disorder, schizophrenia, and healthy aging (Wu et al. 2014; Wu et al. 2016; Bigham et al. 2022; Bigham et al. 2020; Veale et al. 2021; Ji et al. 2019; Phillips et al. 2016; Reginold et al. 2016), among others (Guevara et al. 2020). These findings have been attributed to biological changes such as decreased coherence, decreased axonal packing, and thinning myelin, and further emphasize that SWM is especially affected in various pathologies.

Despite these developments, much is still unknown and uncharacterized about the SWM. For example, features such as the volume occupied by SWM the thickness of the SWM sheet below the cortex have not been characterized. Unlike the cortical thickness and cortical volume metrics that have been thoroughly investigated, are easily quantified using standard toolsets (Fischl 2012; Destrieux et al. 2010), and have proven strong associations with cognition, aging, and disease (Gao et al. 2018; Vogt 2019; Dominguez et al. 2021; Roe et al. 2021; Hou et al. 2021; Dickie et al. 2020; Meyer et al. 2019; Storsve et al. 2016; Fjell and Walhovd 2010; Tustison et al. 2019; Racine et al. 2018; Mattsson et al. 2018; Frangou et al. 2022; Steffener 2021; Habeck et al. 2020), SWM thickness and SWM volume have not been investigated or quantified. Towards this end, we study three high-quality datasets that span the adolescent development, young adulthood, and aging (ages 5–100, N = 2421 subjects), and implement advances and innovations in SWM tractography. First, we quantify total SWM volume and characterize how this tissue volume is associated with age, making comparisons with total brain volume and total white and gray matter tissue volumes. Second, we quantify SWM thickness across the brain, and again describe associations with age in different areas of the brain. Finally, to investigate potential relationships between SWM and neighboring cortex, we explore correlations between SWM features and key features of the overlaying gray matter, including thickness, curvature, and sulcal depth. Together, this effort represents the first characterization of these features of the SWM and how they vary across development, young adulthood, and aging, and provides the background for characterizing normal aging and insight into the mechanisms associated with SWM development and decline.

Methods

This study used three open-sourced datasets that span a large range of the human lifespan (Data), and advances in fiber tractography (Superficial White Matter Tractography) to map features of SWM volume and thickness across the brain (Features and Analysis). With this data, we had four novel aims: (1) characterize SWM thickness across the brain, (2) describe associations between SWM volume and age, (3) describe associations between SWM thickness and age, and (4) quantify relationships between SWM thickness and key cortical features: specifically, thickness, curvature, and sulcal depth.

Because there have been different definitions and descriptions of SWM in the literature, it is important that we define the structures and features we aim to characterize. Here, we defined SWM as white matter that contains short association fibers, or short cortico-cortical connections. We have empirically chosen to define ‘short’ as connections less than 50 mm in length, noting a wide variation described in the literature with short connections ranging from less than 30–35 mm (Schüz et al. 2002; Gao et al. 2014) to less than 80–

85 mm (Guevara et al. 2017; Roman et al. 2017). These short connections form a band, or sheet, immediately adjacent to the cortex. We define the SWM volume as the spatial volume occupied by this band, again noting that due to the complex overlap of white matter pathways in the brain (Schilling 2021) that this volume contains not only short association fibers but also long projecting fibers. Finally, we define SWM thickness as the thickness of this sheet, measuring thickness/length in a direction orthogonal from the cortex and into the white matter. See "Discussion" sections for considerations of SWM definition and associated ambiguity.

Data

The data used in this study come from the Human Connectome Project (Essen et al. 2012), which aims to map the structural connections and circuits of the brain and their relationships to behavior by acquiring high-quality magnetic resonance images. We used diffusion MRI data from the Human Connectome Project Development (HCP-D) study, the Human Connectome Project Young Adult (HCP-YA) study, and the Human Connectome Project Aging (HCP-A) study. HCP-D was composed of 636 subjects with diffusion data, with age ranges between 5 and 21. HCP-YA was composed of 1065 subjects with diffusion data, with age ranges between 21 and 35. HCP-A was composed of 720 subjects with diffusion data, with age ranges between 35 and 100. Thus, the pooled dataset comprised 2421 participants and spanned the ages of 5 and 100. Data demographics are summarized in Table 1 (and distribution of ages given in histogram form in Supplementary Fig. 1).

The diffusion MRI acquisitions were slightly different for each dataset and tailored towards the populations under investigation. For HCP-D and HCP-A, a multi-shell diffusion scheme was used, with b-values of 1500 and 3000 s/mm^2, sampled with 93 and 92 directions, respectively. The in-plane resolution was 1.5 mm, with a slice thickness of 1.5 mm. Susceptibility, motion, and eddy current corrections were performed using TOPUP from the Tiny FSL package (http://github.com/frankyeh/TinyFSL), a re-compiled version of FSL TOPUP (FMRIB, Oxford) with multi-thread support. The corrections were conducted through the integrated interface in DSI Studio's ("Chen" release). For HCP-YA, the minimally preprocessed data (Glasser et al. 2013) from Human Connectome Projects (Q1-Q4 release, 2015) were acquired at Washington University in Saint Louis and the University of Minnesota (Essen et al. 2012) using a multi-shell diffusion scheme, with b-values of 1000, 2000, and 3000 s/mm^2, sampled with 90 directions each. The inplane resolution was 1.25 mm, with a slice thickness of 1.25 mm. Susceptibility, motion, and eddy current corrections were performed as part of the HCP minimal preprocessing pipeline, which also used FSL software TOPUP and EDDY algorithms.

Superficial white matter tractography

For every subject, superficial white matter tractography was performed using methodology similar to Shastin et al. (2022) using MRtrix software (Tournier et al. 2019). Figure 1 shows the reconstruction, tractography, and segmentation pipeline. Briefly, all data were resampled to 1 mm isotropic resolution (using mrgrid command), and multi-shell multi-tissue constrained spherical deconvolution (dwi2fod) (Jeurissen et al. 2014) was performed to derive estimates of the orientation distributions of white matter fibers (Fig. 1, left).

Alignment of diffusion and structural data was performed using a boundary-based rigid registration (epi_reg) from the FSL toolbox (Taki et al. 2011) and subsequently quality checked for accurate alignment. Next, FreeSurfer was performed on the structural T1-weighted images (Lebel et al. 2012) and FreeSurfer's "aseg" volume was transformed to diffusion space to act as input to MRtrix's five tissue type (5TT) image segmentation algorithm (Terribilli et al. 2011). The 5TT image was then manipulated so that cerebellar cortex, amygdala, hippocampus, and deep nuclei were set as gray matter volumes. Thus, upon creation of the white/gray matter boundary for streamline seeding all streamlines are forced to start and end at the neocortex. Tractography was performed using the second-order integration probabilistic algorithm (tckgen) (max angle 45 degrees, step size = 0.5 mm, fODF power = 0.25) (Tournier et al. 2010) to generate 2 million streamlines seeded from the white/gray matter boundary, with a maximum length of 50 mm, using anatomical constraints to ensure gray matter to gray matter connections (Smith et al. 2012), in combination with a number of deep gray matter and deep white matter exclusion zones (Shastin et al. 2022). This pipeline has been shown to yield dense systems of fibers directly below the cortical sheet (Shastin et al. 2022) (Fig. 1, middle). Finally, a tract density map was created (tckmap) (Calamante et al. 2011) at 250 μm isotropic resolution and thresholded at an empirically derived value of three streamlines per voxel (see Discussion on Limitations), resulting in the high-resolution map of the locations of SWM systems (Fig. 1, right).

We performed analyses both using an ROI-based approach and a vertex-based approach with vertices spanning the entire white/gray matter boundary. To this end, the T1-weighted images were analyzed with Freesurfer (Fischl 2012), and results were transformed to diffusion MRI space with ANTs (Avants et al. 2011). From this, we used both the surface file representing the white/gray matter boundary and the Destrieux atlas (Destrieux et al. 2010) parcellation, resulting in 164 neocortical labels for ROI-based analysis.

Features

Two features of the SWM were extracted for this study. First, total SWM volume was calculated based on the SWM segmentation by multiplying the number of voxels within the segmentation by the total voxel volume. SWM volume is a single scalar measure per subject. Second, SWM thickness was calculated for every vertex of the white/gray matter boundary. This was done by querying from the vertex into the white matter (and orthogonal to the white/gray matter boundary) until SWM was no longer detected. This was done in increments of 250 μm until the SWM segmentation was no longer encountered. Once the end of the SWM was reached, two options were possible. If the query point was now within the deep white matter, the distance was entered directly as SWM thickness. If the query point reached gray matter, we divided the traveled distance by two as the measure of SWM thickness. This situation arose primarily along sulcal walls, where SWM of neighboring sulci is not distinguishable within the gyral blade. At the end of this procedure, each vertex of the white/gray matter boundary mesh had an associated SWM thickness, and the average value of each cortical region of interest could be quantified for analysis. This analysis was performed using Matlab (The MathWorks, Natick, MA, USA) and the toolbox provided by FreeSurfer (v7.2.0).

Four cortical features were additionally extracted directly from Freesurfer results: (1) cortical thickness, (2) curvature (sulci have positive curvature, gyri negative, with sharper curvature indicated by higher absolute value), (3) the Jacobian of white matter (which computes how much the white matter surface needs to be distorted to register to the spherical atlas), and (4) sulcal depth (which describes distance from the mid-surface between gyri/sulci; sulci have positive values and gyri have negative values). Note that these features follow FreeSurfer conventions and definitions.

Analysis

Volumetry across age was analyzed using covariate-adjusted restricted cubic spline regression (C-RCS) (Huo et al. 2016), a flexible approach to model nonlinear relationships between variables (using the Covariate-Adjusted Restricted Cubic Spline Regression package available on Matlab Central File Exchange). Here, we used knots at 12, 19, 30, 75, and 90 years of age, based on previously identified developmental shifts in volumetry (Hedman et al. 2012), with five knots being common as a compromise between flexibility and overfitting (Stone 1986). The 95% confidence intervals of volumetric trajectories of each tissue/region of interest are derived by deploying C-RCS regression on 10,000 bootstrap samples. From these samples, the relative change per year (or % change per year) can be calculated as a measure of cross-sectional change. Results were derived binned for age groups pre-determined based on those in the HCP datasets, development (D) (age 5–21), young adult (YA) (21–35), and aging (A) (35–100). To test for a relationship between SWM thickness and features of the cortex across a population for each vertex, using the cortical features of all participants as the independent variable and SWM thickness as the dependent variable, we fit a robust Pearson's correlation coefficient using skipped-correlations (Wilcox 2004) and depicted this cross-sectional correlation coefficient across the brain (Corr_toolbox available on Matlab Central File Exchange). We note that similar results were obtained using traditional Pearson's correlation coefficient (data not shown).

Results

SWM thickness varies across the brain, with patterns robust across individuals and across the population

We begin by examining SWM thickness in individual subjects to highlight not only individual differences, but also show the subject-level data and results that population analysis is based on. Figure 2 shows the SWM segmentation (top), the ROI-based SWM thickness (middle), and the vertex-based SWM thickness (bottom) for three randomly selected subjects in the HCP-D, HCP-YA, and HCP-A cohorts at approximately the median age of each cohort. Qualitatively, SWM runs immediately below and adjacent to the cortex in the expected geometries and locations described in the literature (Guevara et al. 2020; Zhang et al. 2018; Phillips et al. 2013; Oishi et al. 2008). Averaged within gyral regions, SWM thickness largely falls between 2 and 4.5 mm throughout the brain. Vertex-based measures show a much wider range, ranging from < 0.5 mm to some vertices indicating SWM thickness > 10 mm. However, the modes of these distributions in individuals were ~ 1.25–1.5 mm in thickness, with the interquartile range falling within ~ 1.3–3.8 mm. Both vertex-based and ROI-based visualizations indicate moderate hemispheric symmetry on an

individual basis, along with general patterns of high SWM thickness in the frontal lobe, in particular the precentral gyrus and superior frontal cortex, with lower thickness in the temporal and parietal lobes.

We next ask what the SWM thickness looks like averaged across the population, and visualize this for the D, YA, and A cohorts separately in Fig. 3. Here, hemispheric symmetry is much more apparent. Average values again fall largely between 2 and 4 mm with a wider range in the finely grained vertex-averaged values. In the ROI-averaged image, similar spatial patterns of thickness are observed across lobes and gyri, and temporal patterns qualitatively suggest an increase between children and young adults, with small changes into aging that vary slightly by location. In the vertex analysis, the gyral crowns result in a greater thickness measurement than walls or fundi, which is likely a result of the chosen quantification procedure. Notably, throughout both gyri and sulci, higher SWM thickness values are observed again in the frontal lobes and throughout the occipital lobes.

SWM volume shows unique volumetric trajectories with age

Changes in volume for the whole brain, gray matter, white matter, and SWM are shown in Fig. 4 (top), with the relative volume change (%/year) of all tissue types summarized in Fig. 5. Total brain size decreases with age beginning in childhood, (note our cohort starts at 5 years of age) (Hedman et al. 2012; Bethlehem et al. 2022; Takao et al. 2012; Scahill et al. 2003; Taki et al. 2011). Similarly, gray matter volume also decreases with age, with gray matter decreasing faster throughout development and early young adulthood. Also as previously described in the literature, white matter volume increases throughout adolescence, reaching peak volume between 20 and 35 years of age (Bethlehem et al. 2022; Lebel et al. 2012). Here, for the first time, we find that SWM volume shows a similar trend as overall white matter volume, peaking at a similar time in adolescence, leveling off and eventually decreasing throughout adulthood.

The tissue changes relative to whole brain volume show intuitive changes (Fig. 4; middle) (Hedman et al. 2012; Takao et al. 2012; Taki et al. 2011; Terribilli et al. 2011). The % gray matter decreases initially until young adulthood then remains relatively constant throughout life, while white matter again increases, reaching a peak value relative to the whole brain throughout mid-life, then decreases with age. However, the % SWM indicates continual increases with age.

Finally, the percentage of white matter occupied by SWM is plotted (Fig. 4; bottom). SWM occupies a majority of the white matter volume, with the % occupied showing a slight decrease during development, and a small but gradual increase with aging.

SWM thickness shows cross-sectional differences between development, young adult, and aging cohorts that vary across regions

Figure 6 visualizes the percent change per year in SWM thickness, averaged across the cohorts for D (5–21 years old), YA (21–35), and A (35–100) shown for both ROI-based and vertex-based thickness measures. The most pronounced increase in SWM thickness is observed from age 5–21, with widespread positive associations with age increasing by ~ 1–1.5% per year. Prominent cross-sectional changes are seen in the frontal, temporo-parietal,

and superior temporal gyri. In vertex-wise visualizations, this change is observed throughout the gyral crowns, sulcal walls, and fundi, but is most conspicuous at the gyral crowns. SWM thickness shows similar patterns of increases—albeit of a smaller magnitude—from 21 to 35, and levels off or decreases thereafter.

SWM thickness show cross-sectional relationships with key cortical features

To investigate the relationships between SWM thickness and important cortical features (or Freesurfer metrics computed on the cortical surface)—thickness, curvature, Jacobian of the white matter, and sulcal depth—we assessed relationships between features across individuals for every vertex of the surface mesh and visualized the results as cross-sectional correlation coefficients. There was a moderate correlation between cortical thickness and SWM thickness throughout the brain, in both gyri and sulci (Fig. 7), with a correlation coefficient typically greater than 0.2. Thus, as cortical thickness increases, so does SWM thickness. Results for curvatures show unique patterns, with positive values in the prefrontal, temporal, and occipital lobes, and negative correlations in the pre and post central gyri and superior temporal gyri. The Jacobian of the white matter (a measure of how much the white matter surface was distorted to register to an average atlas during process, i.e., a larger value indicates larger distortion) shows weak, but positive, correlations with SWM thickness, with correlations localized to the gyral crowns, indicating that areas which required larger deformations during transformation to a standard space also have larger SWM thicknesses. Finally, sulcal depth shows both positive and negative correlations, with patterns similar to that of curvature.

Discussion

Using a large, high-quality, diffusion MRI dataset, along with innovations in tractography and quantification, we characterized SWM in the human brain across most of the lifespan. Our main findings are that (1) SWM thickness shows patterns robust across individuals and across the population at the region-level and vertex-level, (2) SWM volumetric trajectories with age are distinct from gray matter and total white matter trajectories, (3) SWM shows spatially varying nonlinear changes across the lifespan, and (4) SWM thickness is associated with various features of the corresponding cortex. These findings are discussed in detail below.

SWM volume and age

The brain is known to undergo significant changes during the lifespan. Studies of brain volume, white and gray matter tissue volume (Fjell and Walhovd 2010; Steffener 2021; Hedman et al. 2012; Scahill et al. 2003; Lebel et al. 2012; Fan et al. 2019; Pfefferbaum et al. 1992), cortical thickness (Dominguez et al. 2021; Hou et al. 2021; Frangou et al. 2022; Habeck et al. 2020), microstructure measures (Storsve et al. 2016; Lebel et al. 2012; Fan et al. 2019; Beck et al. 2021), and myelination (Grydeland et al. 2019) have described patterns of neuroanatomical variation that provide insight into the biological sequelae of development and aging. For example, well characterized waves of brain growth occur, with gray matter volume increasing until middle childhood (~ 6 years), followed by volume decreases from young adulthood and into late adulthood, while white matter reaches peak

volume in adulthood (20–40 years), again leveling off and decreasing into late adulthood, with both tissues experiencing accelerated atrophy during late adulthood (Hedman et al. 2012; Bethlehem et al. 2022; Scahill et al. 2003; Lebel et al. 2012). Within each tissue type, changes are heterogenous, with different growth trajectories in different cortical regions and white matter pathways (Lebel et al. 2012; Lebel et al. 2008; Schilling et al. 2022a), and different associations with axonal myelination (Grydeland et al. 2019) and densities (Beck et al. 2021; Schilling et al. 2022a; Cox et al. 2016; Giorgio et al. 2010). These studies have driven hypotheses that aim to relate structure and function and determine structural mediators or cognition (Frangou et al. 2022; Winter et al. 2021; Armstrong et al. 2020), or may serve as a benchmark of normative trajectories that might be used to reveal patterns of abnormal variation or vulnerability in disease and disorder (Fjell and Walhovd 2010; Bethlehem et al. 2022; Shafer et al. 2022).

However, similar studies of SWM have not previously been performed, and measurements of SWM volume and thickness have not been documented. Here, we find that SWM volume trends closely follow those of the total white matter, increasing in volume until young-adulthood during which it levels off and decreases, followed by accelerated decline into late-adulthood. Notably, the relative fraction of total brain volume of these SWM systems increases continually with age, and consequently takes up a larger proportion of total white matter volume, which decreases with respect to total brain volume. While this could be an artifact of processing and tractography (see Limitations, below), it could also indicate relative preservation of these heavily myelinated systems in older age. The fact that our tractography-derived volume fraction estimates (~ 70%) are well in line with existing literature (> 60%) serves as an indirect validation of this quantification. A future study could investigate the sensitivity of these SWM metrics to changes in cognition or mobility as a biomarker for abnormal degeneration, and compare the results against traditional cortical or white matter phenotypes.

SWM thickness

We have additionally shown that SWM thickness shows unique patterns across the brain, in both individuals and across the population. Thicker SWM values tend to be observed in the frontal and occipital lobes, most prominently in precentral gyri and superior frontal gyri of both hemispheres. This is visible both in ROI-averaged and vertex-based maps, although vertex-based maps suggest large variations within a gyrus. While there is noticeable variation of SWM thickness, most of the brain, for most ages, falls within 2–3.5 mm when averaged across entire regions of interest (ranging from < 1 mm to > 10 mm in vertex-based analysis), roughly the same as cortical thickness measures which range between 1 and 5 mm with an average of around 2.5 mm (Fischl and Dale 2000). This estimate is thicker than that provided by susceptibility weighting with estimates of 0.5–2 mm thick (Kirilina et al. 2020), which could represent an overestimation due to larger diffusion MRI voxels, or an underestimation from susceptibility, which is based on only the densest band of T2 relaxometry measures. While this dense band is indeed very thin, observations of histological slices show U-shaped fibers tangential to the sulcal fundi extending beyond this thin band (see Fig. 4 of Reveley et al. (2015), for example). Reassuringly, measures within individuals show modes of the distributions at approximately ~ 1.25–1.5 mm, well in line

with that from other modalities. The averaging across entire gyral blades may bias measures due to quantification at gyral crowns (see Limitations). Moreover, our SWM volumetry measures of ~ 70% of total white matter volume are in line with existing literature of > 60% based on histology (Schüz et al. 2002).

We found that SWM thickness increases throughout the brain across childhood and adolescence, changing at a rate of 1–1.5% per year. The greatest increases occur in the primary motor and sensory areas, with large changes distributed throughout the frontal and occipital lobes, and superior temporal gyri. This perfectly matches the most heavily myelinated areas of the cortex (as derived from T1-weighted over T2-weighted ratios (Grydeland et al. 2019; Glasser and Essen 2011), regions of greatest myelin maturation (Grydeland et al. 2019) (see Figs. 1 and 3 from Grydeland et al. (2019)), and also the areas that show the greatest decline in cortical thickness during the same age period (see Fig. 3 from Frangou et al. (2022)). While all MRI studies may be susceptible to a partial volume effect between cortex and SWM, this suggests a strong temporal relationship between these regions, with increasing myelination, increasing SWM volume, and decreasing cortical thickness. The rates decrease during adulthood; however, the same regions stand out as increasing in thickness with age. These results align with previous studies of the long-range association and projection pathways, where fronto-temporal connections experienced both prolonged development (peaking between 20 and 40 years of age) and late decline. Thus, there is also a complex interplay between the short- and long-range fibers with similar terminal areas. Finally, the rates decline in late aging, although at a much smaller magnitude. However, it is these declines that should be studied, both in terms of volumetric and microstructure-based features (Phillips et al. 2016; Phillips et al. 2013; Schilling et al. 2022b), as they relate to normal and abnormal aging.

Relationship with gray matter

Finally, we show that SWM thickness has unique relationships with features of the cortex. For example, thicker SWM occur in regions of greater cortical thickness. This phenomenon has not been described previously, but reveals an intuitive relationship whereby subjects with greater cortical thickness in a given region also have a larger number of short fibers in this region. The results of positive relationships between SWM thickness and the FreeSurfer derived Jacobian of the white matter serves as a validation that larger SWM requires greater white matter distortion to match the template surface. Finally, curvature and sulcal depth (which are intimately related in that sulci have positive depth and positive curvature, while gyral crowns have negative depth and negative curvature) show unique patterns that vary across the brain. In the precentral and postcentral gyri and superior temporal gyrus, SWM thicknesses are negatively correlated with both (i.e., subjects with greater curvature have thinner SWM), whereas the rest of the brain has positive correlations with both (i.e., subjects with less curvature have thicker SWM). Thus, further investigation is warranted to determine whether this mixed pattern of positive and negative correlations changes with age and whether it is related to gyral complexity or spatial constraints during development—or whether it may be a bias in methodology (see below).

Limitations

Several limitations must be acknowledged. First, tractography faces a number of hurdles, such as partial volume effects with other tissue types (Rheault et al. 2020), limitations in resolving crossing fiber populations (Schilling 2017; Jeurissen et al. 2013), particularly at the cortical interface (Reveley et al. 2015), false positive connections (Maier-Hein et al. 2017) due to bottleneck regions in the brain (Schilling 2021; Girard et al. 2020), and gyral biases (Schilling et al. 2018; St-Onge et al. 2018). However, care was taken to use anatomical constraints (Girard et al. 2014), in combination with surface-based seeding, exclusion regions, and high angular resolution tractography following validated methodology (Shastin et al. 2022). Second, the relatively coarse resolution of diffusion MRI may result in an overestimation of volume and thickness, which is moderated in part by high-resolution tract density imaging and subsequent thresholding which gives sub-voxel resolution of fiber trajectories (Calamante et al. 2011; Calamante et al. 2012), although validation against human histological data is needed. Third, thickness quantification may be overly simplistic. We have chosen an intuitive measure, simply propagating into white matter until SWM are no longer detected. While this works well in sulcal fundi, it is not intuitively quantified along walls or gyri (whereas the cortical thickness is well-defined between two tangential surfaces). We have chosen to divide this value by ½ within sulcal walls that project directly to the neighboring sulcal wall (with the assumption that the SWM systems associated with each wall take up approximately half the gyral blade). It is unknown what percentage of fibers within a gyral blade connect to each side of the SWM gyrus, and our solution is clearly only an approximation. This will also lead to overestimates at the top of gyral crowns, where the thickness may truly be a measure of sulcal length. It remains to be investigated how SWM is associated with crowns and whether thickness should be quantified at these locations. Another bias due to methodology is that increased volume fraction of SWM relative to whole brain volume as a function of age could be an artifact of reduced whole brain volume as a function of age and improved ability of tractography to form short connections, both true and false positive connections. Next, different diffusion acquisition and experimental settings are known to influence tractography results (Schilling et al. 2021a), and makes direct comparisons across sites challenging (Ning et al. 2020; Tax 2019; Fortin et al. 2018). For this reason, while the aging trajectories are fit using cubic splines, we have chosen to visualize results within each cohort separately. Additionally, cubic splines may be unstable at the tails, yet cross-sectional trends are well-captured within our cohorts age range. While all choices in the tractography process effect results (Schilling et al. 2021b; Schilling et al. 2021), one such choice is the streamline length. The definition of “superficial white matter” and descriptions of the length of these systems varies in literature. We have chosen a streamline length that sits within the range described in the literature (Guevara et al. 2020; Shastin et al. 2022), but show in supplementary experiments on a subset of this data that trends are consistent within individuals and across individuals regardless of streamline length (supplementary data). Finally, while this study is composed of large, high-quality, datasets covering ages 5–100, it is cross-sectional only—thus, we can only infer cross-sectional associations with age, whereas longitudinal datasets would allow a more powerful analysis of change with age.

Conclusion

SWM represents a significantly understudied part of the human brain, despite taking up a large portion of its volume and making up a majority of its structural connections. Using multiple, high-quality, datasets with large sample sizes in combination with methodological advances in tractography, we quantified changes in SWM across development, young adulthood, and aging. We identified and characterized changes in SWM volume and thickness across these age ranges, describing trajectories that are unique from gray matter and other white matter tissue. SWM thickness varies across the brain, is reproducible across the population, and shows heterogenous changes during development, young adulthood, and aging. Finally, we find that SWM thickness is related to other biological and geometrical features of the brain. Thus, SWM is continuously changing during the lifespan, and studies of these systems, together with gray matter and other white matter features, can provide insight into normal and abnormal development and aging.

Supplementary Material

Refer to Web version on PubMed Central for supplementary material.

Acknowledgements

This work was supported by the National Science Foundation Career Award #1452485, the National Institutes of Health under award numbers R01EB017230, K01EB032898, K01-AG073584, 1 S10OD021771 01, and in part by ViSE/VICTR VR3029 and the National Center for Research Resources, Grant UL1 RR024975–01.

Funding

The authors have not disclosed any funding.

Data availability

The data used in this study come from the Human Connectome Project (Essen et al. 2012), including HCP Young Adult, HCP Aging, and HCP Development cohorts, which are freely available after appropriate data usage agreements. See the following for data download: HCP Young Adult (https://www.humanconnectome.org/study/hcp-young-adult/document/1200-subjects-data-release), HCP Aging and Development (https://nda.nih.gov/general-query.html?q=query=featured-datasets:HCP%20Aging%20and%20Development).

References

Armstrong NM et al. (2020) Associations between cognitive and brain volume changes in cognitively normal older adults. Neuroimage 223:117289 [PubMed: 32835822]

Avants BB et al. (2011) A reproducible evaluation of ANTs similarity metric performance in brain image registration. Neuroimage 54(3):2033–2044 [PubMed: 20851191]

Barkovich AJ (2000) Concepts of myelin and myelination in neuroradiology. AJNR Am J Neuroradiol 21(6):1099–1109 [PubMed: 10871022]

Beck D et al. (2021) White matter microstructure across the adult lifespan: a mixed longitudinal and cross-sectional study using advanced diffusion models and brain-age prediction. Neuroimage 224:117441 [PubMed: 33039618]

Bethlehem RAI et al. (2022) Brain charts for the human lifespan. Nature 604(7906):525–533 [PubMed: 35388223]

Bigham B et al. (2020) Identification of superficial white matter abnormalities in Alzheimer's disease and mild cognitive impairment using diffusion tensor imaging. J Alzheimers Dis Rep 4(1):49–59 [PubMed: 32206757]

Bigham B et al. (2022) Features of the superficial white matter as biomarkers for the detection of Alzheimer's disease and mild cognitive impairment: a diffusion tensor imaging study. Heliyon 8(1):e08725 [PubMed: 35071808]

Calamante F et al. (2011) Track density imaging (TDI): validation of super resolution property. Neuroimage 56(3):1259–1266 [PubMed: 21354314]

Calamante F et al. (2012) Super-resolution track-density imaging studies of mouse brain: comparison to histology. Neuroimage 59(1):286–296 [PubMed: 21777683]

Cox SR et al. (2016) Ageing and brain white matter structure in 3,513 UK Biobank participants. Nat Commun 7:13629 [PubMed: 27976682]

Destrieux C et al. (2010) Automatic parcellation of human cortical gyri and sulci using standard anatomical nomenclature. Neuroimage 53(1):1–15 [PubMed: 20547229]

Dickie DA et al. (2020) Cortical thickness, white matter hyperintensities, and cognition after stroke. Int J Stroke 15(1):46–54 [PubMed: 31088224]

Dominguez EN et al. (2021) Regional cortical thickness predicts top cognitive performance in the elderly. Front Aging Neurosci 13:751375 [PubMed: 34803657]

Fan Q et al. (2019) Age-related alterations in axonal microstructure in the corpus callosum measured by high-gradient diffusion MRI. Neuroimage 191:325–336 [PubMed: 30790671]

Fischl B (2012) FreeSurfer. Neuroimage 62(2):774–781 [PubMed: 22248573]

Fischl B, Dale AM (2000) Measuring the thickness of the human cerebral cortex from magnetic resonance images. Proc Natl Acad Sci USA 97(20):11050–11055 [PubMed: 10984517]

Fjell AM, Walhovd KB (2010) Structural brain changes in aging: courses, causes and cognitive consequences. Rev Neurosci 21(3):187–221 [PubMed: 20879692]

Fortin JP et al. (2018) Harmonization of cortical thickness measurements across scanners and sites. Neuroimage 167:104–120 [PubMed: 29155184]

Frangou S et al. (2022) Cortical thickness across the lifespan: data from 17,075 healthy individuals aged 3–90 years. Hum Brain Mapp 43(1):431–451 [PubMed: 33595143]

Gao J et al. (2014) The relevance of short-range fibers to cognitive efficiency and brain activation in aging and dementia. PLoS One 9(4):e90307 [PubMed: 24694731]

Gao Y et al. (2018) Changes in cortical thickness in patients with early Parkinson's disease at different hoehn and yahr stages. Front Hum Neurosci 12:469 [PubMed: 30542273]

Giorgio A et al. (2010) Age-related changes in grey and white matter structure throughout adulthood. Neuroimage 51(3):943–951 [PubMed: 20211265]

Girard G et al. (2014) Towards quantitative connectivity analysis: reducing tractography biases. Neuroimage 98:266–278 [PubMed: 24816531]

Girard G et al. (2020) On the cortical connectivity in the macaque brain: a comparison of diffusion tractography and histological tracing data. Neuroimage 221:117201 [PubMed: 32739552]

Glasser MF, Van Essen DC (2011) Mapping human cortical areas in vivo based on myelin content as revealed by T1- and T2-weighted MRI. J Neurosci 31(32):11597–11616 [PubMed: 21832190]

Glasser MF et al. (2013) The minimal preprocessing pipelines for the human connectome project. Neuroimage 80:105–124 [PubMed: 23668970]

Grydeland H et al. (2019) Waves of maturation and senescence in micro-structural MRI markers of human cortical myelination over the lifespan. Cereb Cortex 29(3):1369–1381 [PubMed: 30590439]

Guevara M et al. (2017) Reproducibility of superficial white matter tracts using diffusion-weighted imaging tractography. Neuroimage 147:703–725 [PubMed: 28034765]

Guevara M et al. (2020) Superficial white matter: a review on the dMRI analysis methods and applications. Neuroimage 212:116673 [PubMed: 32114152]

Habeck C et al. (2020) Cortical thickness and its associations with age, total cognition and education across the adult lifespan. PLoS One 15(3):e0230298 [PubMed: 32210453]

Hedman AM et al. (2012) Human brain changes across the life span: a review of 56 longitudinal magnetic resonance imaging studies. Hum Brain Mapp 33(8):1987–2002 [PubMed: 21915942]

Hou M et al. (2021) Specific and general relationships between cortical thickness and cognition in older adults: a longitudinal study. Neurobiol Aging 102:89–101 [PubMed: 33765434]

Huo Y et al. (2016) Mapping lifetime brain volumetry with covariate-adjusted restricted cubic spline regression from cross-sectional multi-site MRI. Med Image Comput Comput Assist Interv 9900:81–88 [PubMed: 28191550]

Jeurissen B et al. (2013) Investigating the prevalence of complex fiber configurations in white matter tissue with diffusion magnetic resonance imaging. Hum Brain Mapp 34(11):2747–2766 [PubMed: 22611035]

Jeurissen B et al. (2014) Multi-tissue constrained spherical deconvolution for improved analysis of multi-shell diffusion MRI data. Neuroimage 103:411–426 [PubMed: 25109526]

Jeurissen B et al. (2019) Diffusion MRI fiber tractography of the brain. NMR Biomed 32(4):e3785 [PubMed: 28945294]

Ji E et al. (2019) Increased and decreased superficial white matter structural connectivity in schizophrenia and bipolar disorder. Schizophr Bull 45(6):1367–1378 [PubMed: 30953566]

Kirilina E et al. (2020) Superficial white matter imaging: Contrast mechanisms and whole-brain in vivo mapping. Sci Adv. 10.1126/sciadv.aaz9281

Lebel C et al. (2008) Microstructural maturation of the human brain from childhood to adulthood. Neuroimage 40(3):1044–1055 [PubMed: 18295509]

Lebel C et al. (2012) Diffusion tensor imaging of white matter tract evolution over the lifespan. Neuroimage 60(1):340–352 [PubMed: 22178809]

Maier-Hein KH et al. (2017) The challenge of mapping the human connectome based on diffusion tractography. Nat Commun 8(1):1349 [PubMed: 29116093]

Maricich SM et al. (2007) Myelination as assessed by conventional MR imaging is normal in young children with idiopathic developmental delay. Am J Neuroradiol 28(8):1602 [PubMed: 17846220]

Mattsson N et al. (2018) Greater tau load and reduced cortical thickness in APOE epsilon4-negative Alzheimer's disease: a cohort study. Alzheimers Res Ther 10(1):77 [PubMed: 30086796]

Meyer K et al. (2019) Are global and specific interindividual differences in cortical thickness associated with facets of cognitive abilities, including face cognition? R Soc Open Sci 6(7):180857 [PubMed: 31417686]

Ning L et al. (2020) Cross-scanner and cross-protocol multi-shell diffusion MRI data harmonization: algorithms and results. Neuroimage 221:117128 [PubMed: 32673745]

Oishi K et al. (2008) Human brain white matter atlas: identification and assignment of common anatomical structures in superficial white matter. Neuroimage 43(3):447–457 [PubMed: 18692144]

Pfefferbaum A et al. (1992) Brain gray and white matter volume loss accelerates with aging in chronic alcoholics: a quantitative MRI study. Alcohol Clin Exp Res 16(6):1078–1089 [PubMed: 1471762]

Phillips OR et al. (2013) Superficial white matter: effects of age, sex, and hemisphere. Brain Connect 3(2):146–159 [PubMed: 23461767]

Phillips OR et al. (2016) The superficial white matter in Alzheimer's disease. Hum Brain Mapp 37(4):1321–1334 [PubMed: 26801955]

Racine AM et al. (2018) The personalized Alzheimer's disease cortical thickness index predicts likely pathology and clinical progression in mild cognitive impairment. Alzheimers Dement (amst) 10:301–310 [PubMed: 29780874]

Reginold W et al. (2016) Altered superficial white matter on tractography MRI in Alzheimer's disease. Dement Geriatr Cogn Dis Extra 6(2):233–241 [PubMed: 27489557]

Reveley C et al. (2015) Superficial white matter fiber systems impede detection of long-range cortical connections in diffusion MR tractography. Proc Natl Acad Sci USA 112(21):E2820–E2828 [PubMed: 25964365]

Rheault F et al. (2020) Common misconceptions, hidden biases and modern challenges of dMRI tractography. J Neural Eng 17(1):011001 [PubMed: 31931484]

Roe JM et al. (2021) Asymmetric thinning of the cerebral cortex across the adult lifespan is accelerated in Alzheimer's disease. Nat Commun 12(1):721 [PubMed: 33526780]

Roman C et al. (2017) Clustering of whole-brain white matter short association bundles using HARDI data. Front Neuroinform 11:73 [PubMed: 29311886]

Scahill RI et al. (2003) A longitudinal study of brain volume changes in normal aging using serial registered magnetic resonance imaging. Arch Neurol 60(7):989–994 [PubMed: 12873856]

Schilling K et al. (2017) Can increased spatial resolution solve the crossing fiber problem for diffusion MRI? NMR Biomed 30(12):e3787

Schilling K et al. (2018) Confirmation of a gyral bias in diffusion MRI fiber tractography. Hum Brain Mapp 39(3):1449–1466 [PubMed: 29266522]

Schilling KG et al. (2021) Prevalence of white matter pathways coming into a single white matter voxel orientation: the bottleneck issue in tractography. Hum Brain Mapp 14:82

Schilling KG et al. (2021) Fiber tractography bundle segmentation depends on scanner effects, acquisition, diffusion sensitization, and bundle segmentation workflow. bioRxiv 32:e3241

Schilling KG et al. (2021a) Fiber tractography bundle segmentation depends on scanner effects, vendor effects, acquisition resolution, diffusion sampling scheme, diffusion sensitization, and bundle segmentation workflow. Neuroimage 242:118451 [PubMed: 34358660]

Schilling KG et al. (2021b) Tractography dissection variability: What happens when 42 groups dissect 14 white matter bundles on the same dataset? Neuroimage 243:118502 [PubMed: 34433094]

Schilling K et al. (2022a) Aging and white matter microstructure and macrostructure: a longitudinal multi-site diffusion MRI study of 1,184 participants. bioRxiv 183:239

Schilling KG et al. (2022b) Short superficial white matter and aging: a longitudinal multi-site study of 1,293 subjects and 2,711 sessions. bioRxiv 3:100067

Schüz A, Miller R (2002) Cortical areas: unity and diversity. Taylor & Francis, London, p 520

Schüz A, Braitenberg V, Miller R (2002) The human cortical white matter: quantitative aspects of cortico-cortical long-range connectivity. In: Schüz A, Miller R (eds) Cortical areas: unity and diversity. CRC Press, Boco Raton, pp 377–385

Schuz A et al. (2006) Quantitative aspects of corticocortical connections: a tracer study in the mouse. Cereb Cortex 16(10):1474–1486 [PubMed: 16357338]

Shafer AT et al. (2022) Accelerated decline in white matter microstructure in subsequently impaired older adults and its relationship with cognitive decline. Brain Commun 4(2):fcac051 [PubMed: 35356033]

Shastin D et al. (2022) Surface-based tracking for short association fibre tractography. Neuroimage 260:119423 [PubMed: 35809886]

Smith RE et al. (2012) Anatomically-constrained tractography: improved diffusion MRI streamlines tractography through effective use of anatomical information. Neuroimage 62(3):1924–1938 [PubMed: 22705374]

Steffener J (2021) Education and age-related differences in cortical thickness and volume across the lifespan. Neurobiol Aging 102:102–110 [PubMed: 33765423]

Stone CJ (1986) [Generalized additive models]: comment. Stat Sci 1(3):312–314

St-Onge E et al. (2018) Surface-enhanced tractography (SET). Neuroimage 169:524–539 [PubMed: 29258891]

Storsve AB et al. (2016) Longitudinal changes in white matter tract integrity across the adult lifespan and its relation to cortical thinning. PLoS One 11(6):e0156770 [PubMed: 27253393]

Suarez-Sola ML et al. (2009) Neurons in the white matter of the adult human neocortex. Front Neuroanat 3:7 [PubMed: 19543540]

Takao H, Hayashi N, Ohtomo K (2012) A longitudinal study of brain volume changes in normal aging. Eur J Radiol 81(10):2801–2804 [PubMed: 22104089]

Taki Y et al. (2011) A longitudinal study of gray matter volume decline with age and modifying factors. Neurobiol Aging 32(5):907–915 [PubMed: 19497638]

Tax CM et al. (2019) Cross-scanner and cross-protocol diffusion MRI data harmonisation: a benchmark database and evaluation of algorithms. Neuroimage 195:285 [PubMed: 30716459]

Terribilli D et al. (2011) Age-related gray matter volume changes in the brain during non-elderly adulthood. Neurobiol Aging 32(2):354–368 [PubMed: 19282066]

Tournier JD, Calamante F, Connelly A (2010) Improved probabilistic streamlines tractography by 2nd order integration over fibre orientation distributions. Proc. Intl. Soc. Mag. Reson. Med. (ISMRM). 18

Tournier JD et al. (2019) MRtrix3: a fast, flexible and open software framework for medical image processing and visualisation. Neuroimage 202:116137 [PubMed: 31473352]

Tustison NJ et al. (2019) Longitudinal mapping of cortical thickness measurements: an Alzheimer's disease neuroimaging initiative-based evaluation study. J Alzheimers Dis 71(1):165–183 [PubMed: 31356207]

Van Essen DC et al. (2012) The human connectome project: a data acquisition perspective. Neuroimage 62(4):2222–2231 [PubMed: 22366334]

Veale T et al. (2021) Loss and dispersion of superficial white matter in Alzheimer's disease: a diffusion MRI study. Brain Commun 3(4):fcab272 [PubMed: 34859218]

Vogt NM et al. (2019) Cortical microstructural alterations in mild cognitive impairment and Alzheimer's disease dementia. Cereb Cortex 30:2948

Wilcox R (2004) Inferences based on a skipped correlation coefficient. J Appl Stat 31(2):131–143

Winter M et al. (2021) Tract-specific MRI measures explain learning and recall differences in multiple sclerosis. Brain Commun. 10.1093/braincomms/fcab065

Wu M et al. (2014) Development of superficial white matter and its structural interplay with cortical gray matter in children and adolescents. Hum Brain Mapp 35(6):2806–2816 [PubMed: 24038932]

Wu M, Kumar A, Yang S (2016) Development and aging of superficial white matter myelin from young adulthood to old age: mapping by vertex-based surface statistics (VBSS). Hum Brain Mapp 37(5):1759–1769 [PubMed: 26955787]

Zhang F et al. (2018) An anatomically curated fiber clustering white matter atlas for consistent white matter tract parcellation across the lifespan. Neuroimage 179:429–447 [PubMed: 29920375]

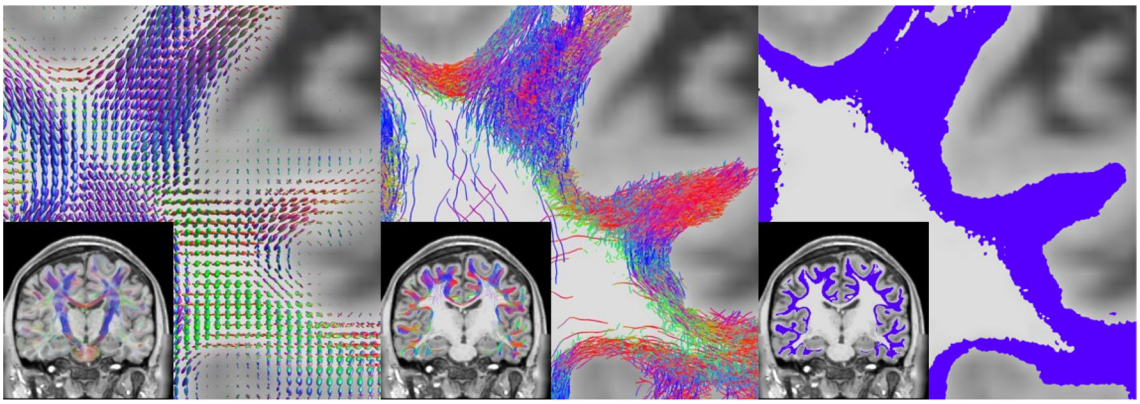

Fig. 1.

Superficial white matter tractography was performed using methodology similar to Shastin et al. (2022) in order to derive SWM segmentations. This included multi-shell multi-tissue spherical deconvolution (Jeurissen et al. 2014) to derive fiber orientation distributions (left), anatomically informed probabilistic tractography (Tournier et al. 2010) and filtering (middle), and tract segmentation (right)

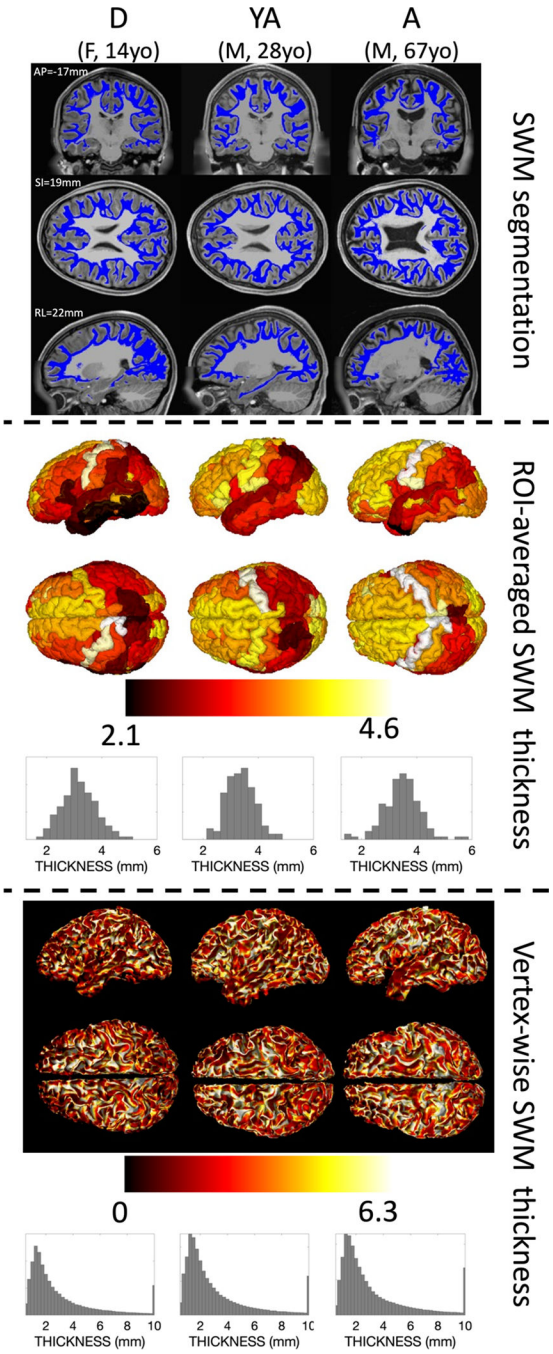

Fig. 2.

Qualitative differences in SWM thickness are visible across the brain and across the lifespan in individual subjects. SWM segmentation (top), ROI-average SWM thickness (middle), and vertex-wise SWM thickness (bottom) are shown for three randomly selected subjects at approximately the median age from the development (D), young adult (YA), and aging (A) cohorts. Coordinates are given in MNI305 space and are the same across subjects, and additional views are given in supplementary information

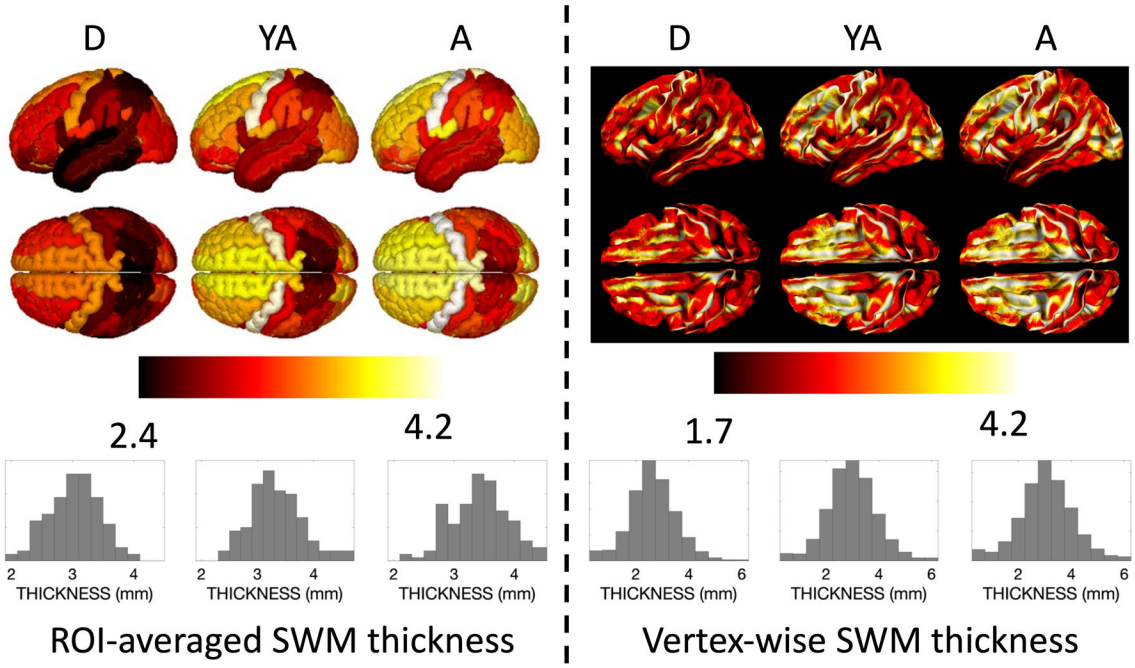

Fig. 3.

Qualitative differences in SWM thickness are visible across the brain and across the lifespan for the population-averaged subjects for each cohort. The average ROI-based SWM thickness (left) and vertex-based SWM thickness (right) is shown for each of the development (D), young adult (YA), and aging (A) cohorts. ROI names (from Destrieux atlas) and associated population-averaged SWM thickness for each cohort are given in supplementary data, along with additional views of the brain

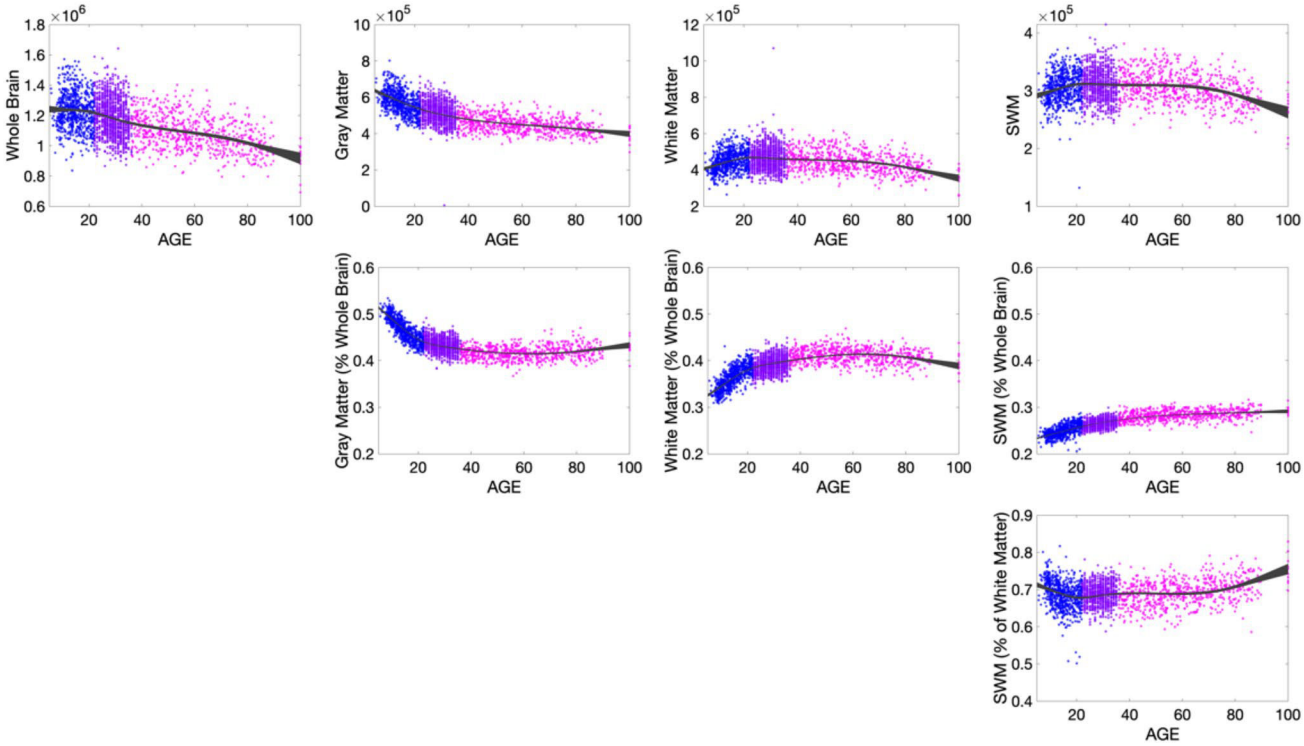

Fig. 4.

SWM shows volumetric trajectory with age that is unique from total white matter and total gray matter volumes. Row 1 shows the volumetric changes in total brain volume, gray matter, white matter, and SWM volumes. Row 2 shows changes relative to whole brain volume, and Row 3 shows the changes in SWM relative to total white matter volume. Points are colored based on dataset to emphasize and highlight age ranges from the non-overlapping cohorts: HCP D (5–22), HCP YA (22–35), HCP A (35 +)

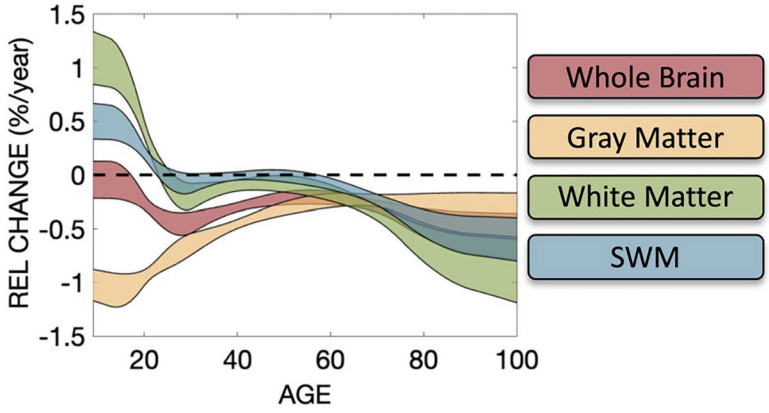

Fig. 5.

Relative volume change in % change per year for whole brain, gray matter, white matter, and SWM tissue types. 95% confidence intervals in all plots are calculated from 10,000 bootstrap samples, with 0% (i.e., no change) as solid dashed line. Note white matter and SWM trends crossing 0 indicate peak in volume

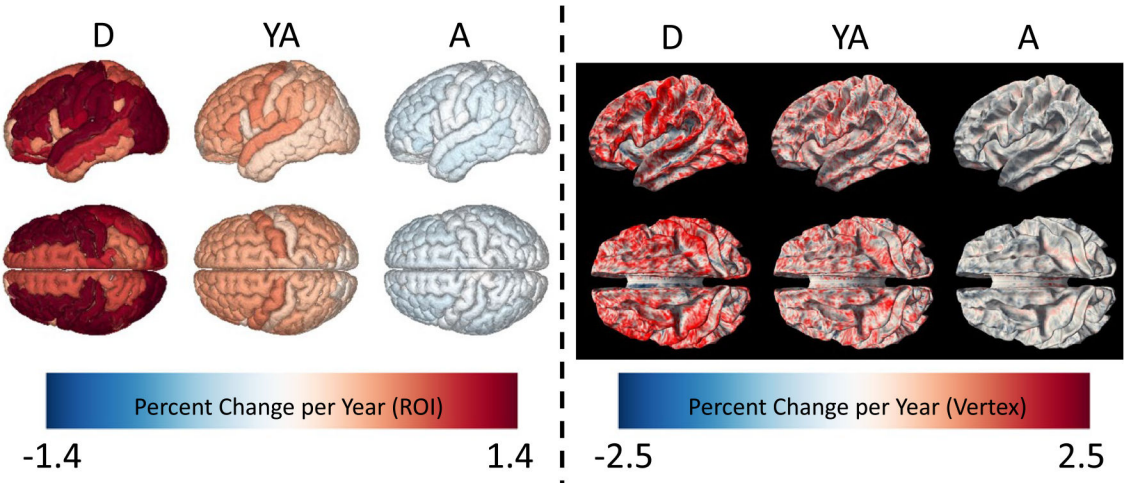

Fig. 6.

SWM thickness shows cross-sectional changes across development, young adulthood, and aging, with change dependent on location. Left shows ROI-based analysis colored by percent change per year for D, YA, and A cohorts. Right shows the vertex-based analysis colored by percent change per year for the same cohorts. Additional views are given in supplementary information

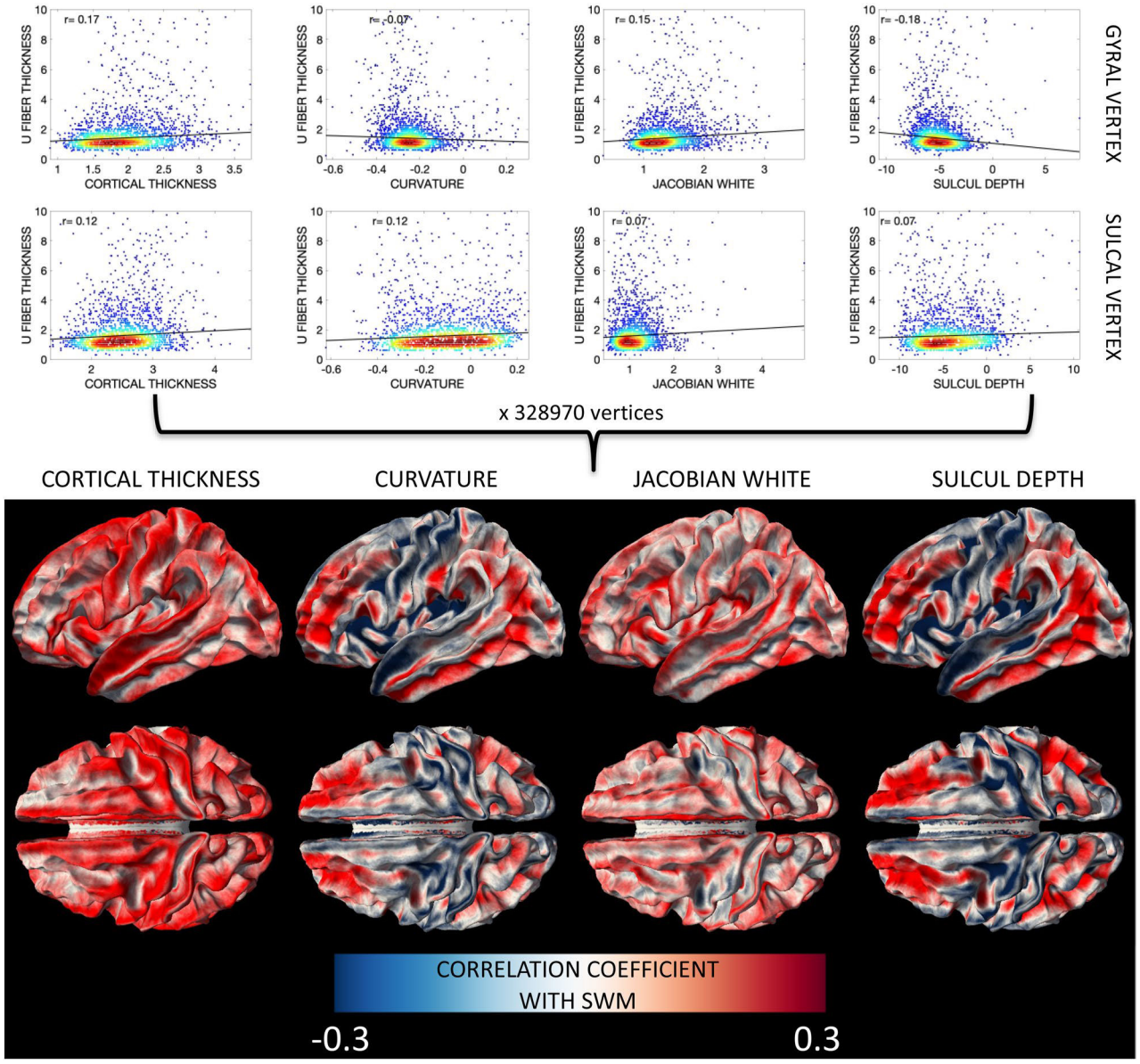

Fig. 7.

SWM thickness shows cross-sectional relationships with FreeSurfer-defined features of the cortex (cortical thickness, curvature, Jacobian of the white matter, and sulcal depth) that vary based on brain location. Here, for every vertex, a robust correlation coefficient between SWM thickness and cortical feature across the population was calculated (plots shown in bottom row) and displayed on the white/gray matter boundary for all vertices (top row). Results separated by age group are given in supplementary information

Table 1

Data used in this study come from the Human Connectome Project (Essen et al. 2012) initiatives—the Human Connectome Project Development (HCP-D) study, the Human Connectome Project Young Adult (HCP-YA) study, and the Human Connectome Project Aging (HCP-A) study

	HCP D	HCP YA	HCP A	Total
Subjects	636	1065	720	2421
Age Range	[5.5 21.9]	[22 35]	[36 100]	[5.5 100]
Age	14.4 ± 4.0	28.8 ± 3.5	60.4 ± 15.6	34.0 ± 19.6
Sex	341 F; 295M	575F; 490M	402F; 318M	1318F; 1103M

Age is presented as mean ± standard deviation. Sex and age are available through HCP Open Access Data Use Terms